Separation Science and Technology
Publication details, including instructions for authors and subscription information:
http://www.informaworld.com/smpp/title~content=t713708471

Continuous Particle Electrophoresis: A New Analytical and Preparative Capability

Allen Strickler[a]
[a] Advanced Technology Operations Beckman Instruments, Inc, Fullerton, California

To cite this Article Strickler, Allen(1967) 'Continuous Particle Electrophoresis: A New Analytical and Preparative Capability', Separation Science and Technology, 2: 3, 335 — 355
To link to this Article: DOI: 10.1080/01496396708049706
URL: http://dx.doi.org/10.1080/01496396708049706

SEPARATION SCIENCE, 2(3), 335–355 (1967)

Continuous Particle Electrophoresis: A New Analytical and Preparative Capability*

ALLEN STRICKLER
ADVANCED TECHNOLOGY OPERATIONS
BECKMAN INSTRUMENTS, INC.
FULLERTON, CALIFORNIA

Summary

New differential migration techniques are breaching a barrier in terms of particle size in mixtures to be fractionated. Thus electrophoresis in free media is being applied to a wide variety of particles, mainly of biological interest, ranging from viruses to whole tissue cells and from 100 A to tens of microns in dimensions. A new technique of high-speed continuous electrophoresis is discussed which appears to offer a new order of capability for fractionating and studying of particles. An analysis is presented of certain considerations underlying this capability, in terms of instrument-response time, resolution, and sample-handling rate. Band broadening due to diffusion and velocity-profile effects is discussed in some detail and related to performance. Factors involved in making absolute mobility measurements are considered.

Contemporary separation science has comprised, in the main, an array of powerful techniques of a differential migration type. These typically have the capability of fractionating mixtures of multiple components, and characterizing them by positions in a "spectrum" or pattern which aids identification. In these terms, separation science has been pressing against a kind of dimensional barrier. It has been almost wholly confined to molecularly dispersed components. At its upper limits it has been accommodating macromolecules such as those of proteins with dimensions of the order of 100 Å. This barrier is now beginning to be breached. The tools implementing this progress include density-gradient centrifugation (*1*) and various forms of electrophoresis in free media.

* This article will be published later in a volume entitled *Separation Techniques: Proceedings of the Nineteenth Annual Summer Symposium on Analytical Chemistry.*

These developments come at a time of urgent need. In the fields of molecular and cell biology, a backlog of new separation needs is rapidly accumulating. These involve many particles at a level of organization beyond the macromolecular: viruses, microsomes, mitochondria, chromosomes, chloroplasts, nuclei, bacteria, blood cells, and whole tissue cells. In dimensions, these entities extend from 100 Å for the smallest viruses to tens of microns or larger in many tissue cells. Outside of biology, there remains a long-standing need in the colloidal and related sciences for techniques aiding the separation and study of many particle mixtures. In the following, our attention is directed particularly to electrophoresis in free media as a means for fractionating the various "microparticles."

The electrophoretic behavior of particles is founded in the same general theory (*2,3*) that applies to molecular components. Research experience in particle electrophoresis dates back nearly a half century and has been based on the so-called "microscope technique" (*4*). This involves dispersing the particles in a thin electrolyte layer within a glass cell, applying a d-c field, and observing individual particle velocities under a microscope at specified depths within the cell. The mobility of the particle is a measure of its ζ potential, this being proportional to the charge density at the particle surface, and a function of the dielectric and ionic properties of the medium. The microscope technique has been used extensively in colloidal studies (*3*) and in biology (*4–6*) for the elucidation of particle surface phenomena and particle interaction effects.

Fractionation of microparticles has appeared generally to preclude the use of any support medium. Efforts to achieve a zone electrophoresis of particles have therefore been dominated by problems of stabilization in free liquid media. The disturbing influences are thermal convection and gravitational settling of particles. Kolin, Mel, and Hjertin have variously reported an electromagnetic method of stabilization in which the medium is caused to rotate in an annular gap (*7*), the use of density gradients (*8,9*), and mechanical rotation of a cylindrical electrophoresis tube (*10,11*).

A continuous free film electrophoresis technique for dissolved components, originated by Barrolier (*12*) and further developed by Hannig (*13*), recently (*14*) was adapted and applied by Hanning to the fractionation of certain types of microparticles. It is characterized by a very thin (0.5 mm) curtain and a relatively long curtain residence time (typically 1 hour). This has made difficult the accom-

modation of particles with an appreciable settling rate, and made obligatory the use of a cell cooling system. Also, the broadening effects relative to the rate of sample introduction have appeared quite large.

The following discusses an independent development in continuous free-flow electrophoresis. It appears to offer a new order of capability in particle separations. Our interest originated in a need for a rapid analytical monitoring device for mixtures of microscopic particles. Our hopes were soon fixed on the promise of separation in a miniature, continuous free-film device. This hope was justified when, in late 1963, we were fully resolving bacterial mixtures and various inorganic pigments, apparently for the first time, in a cell 8×10 cm (*15*).

Stabilization against convection and particle settling effects, as well as other important new advantages, was achieved by use of a rapidly flowing, narrow film in a cell of special design. The method avoided the use of density gradients and magnetic fields, and proved to be extraordinarily rapid, giving an electrophoresis pattern in 30 seconds or less from the time of sample injection. Heating effects were minimized by the rapid flow, and in ordinary use special cooling provision for the cell was not required. The short transit time was also favorable for working with sensitive biological particles, since brief exposure to the slightly elevated temperature would not be damaging.

DESCRIPTION

The basic design of the instrument and its performance have been reported earlier (*16*). We therefore present only a brief description here. In the remainder of the article, for the special interest of present readers, we examine some of the considerations underlying the new performance.

Figure 1 illustrates the latest cell design,* as improved by the author's colleague, V. R. Huebner, and co-workers. This development will be described in detail elsewhere.

The cell consists of two plates separated about 1.5 mm by a special gasket assembly. The latter defines a parallel flow space, about 5 cm wide and 30 cm long, between an upper curtain inlet and a lower outlet. Special assemblies fitted to the back plate serve

* Patents applied for.

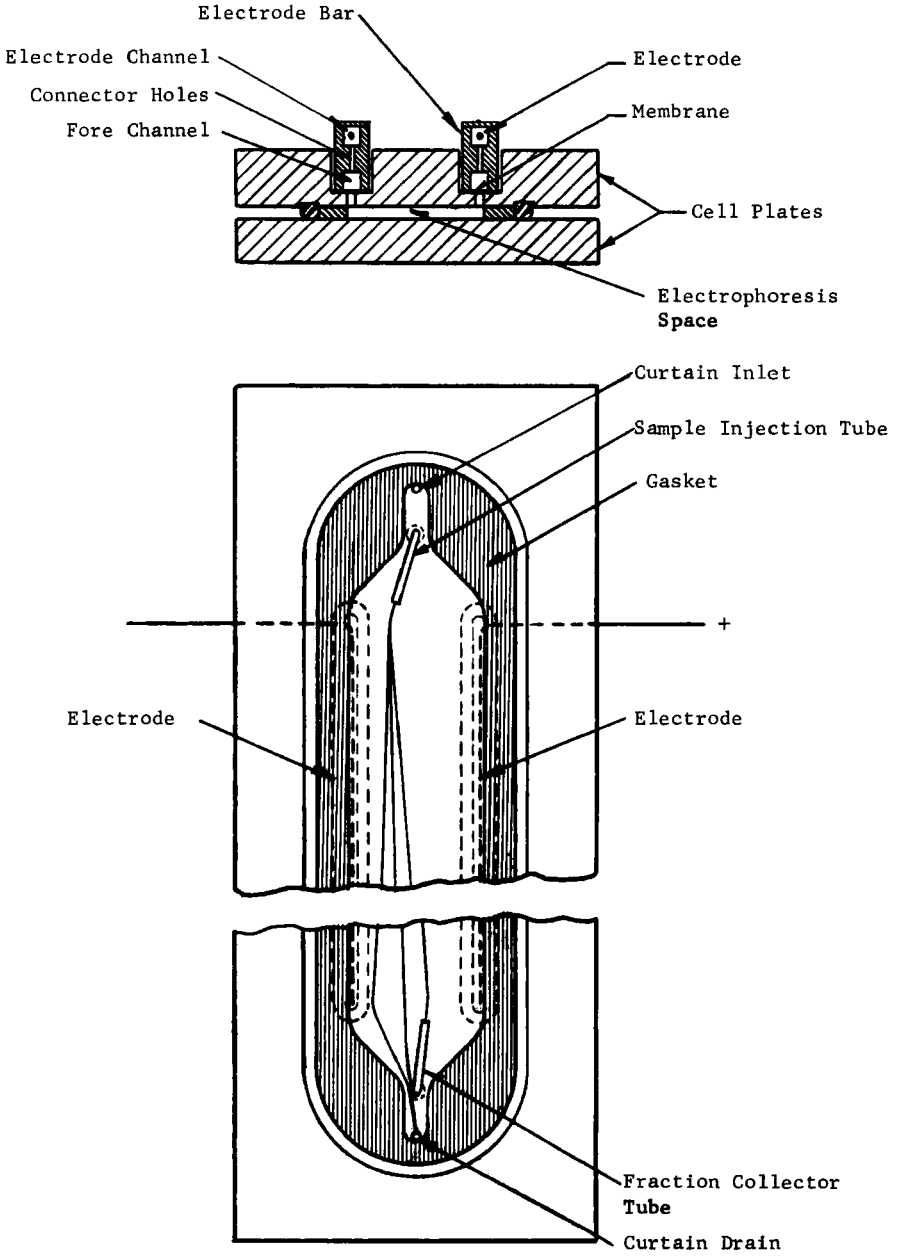

FIG. 1. Cell design.

to couple a pair of electrodes to the edges of flowing curtain. These assemblies provide internal counterflow flushing of the electrodes to prevent migration of electrolysis products into the curtain.

The sample suspension is injected via a fixed tube between the plates (Fig. 2), or via a rotatable tube as shown in Fig. 1. Desired components in the fractionation pattern may be intercepted by a second swivel tube at the bottom of the curtain, and collected ex-

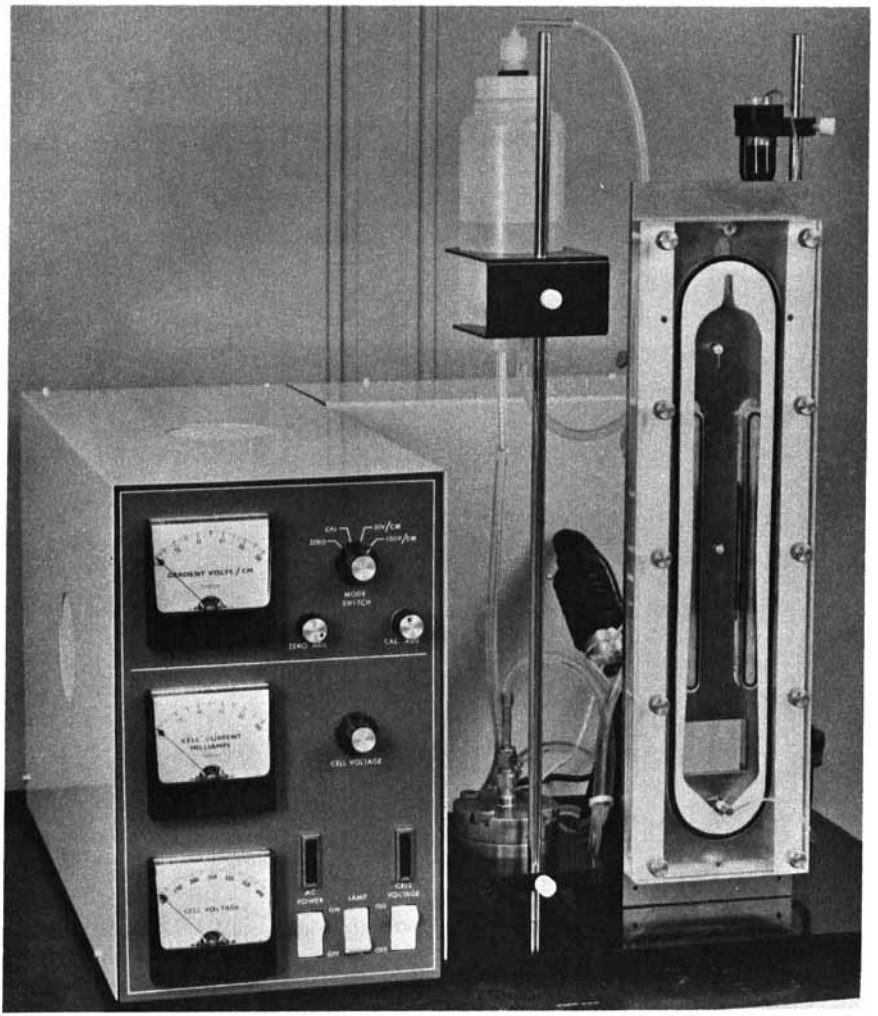

FIG. 2. Continuous particle electrophoresis system.

ternally. In an alternative arrangement (not shown), the curtain may be drained off through an array of tubes and multiple fractions collected simultaneously.

Figure 2 shows the complete instrument. The enclosed section houses the voltage supply, a voltage-gradient measuring circuit, and the reservoirs, pumps, and filter needed to maintain curtain flow and rinse the electrodes.

Curtain flow rate is typically 20 ml/min; typical vertical velocity at the curtain midplane is about 0.5 to 1 cm/sec. Sample flow may

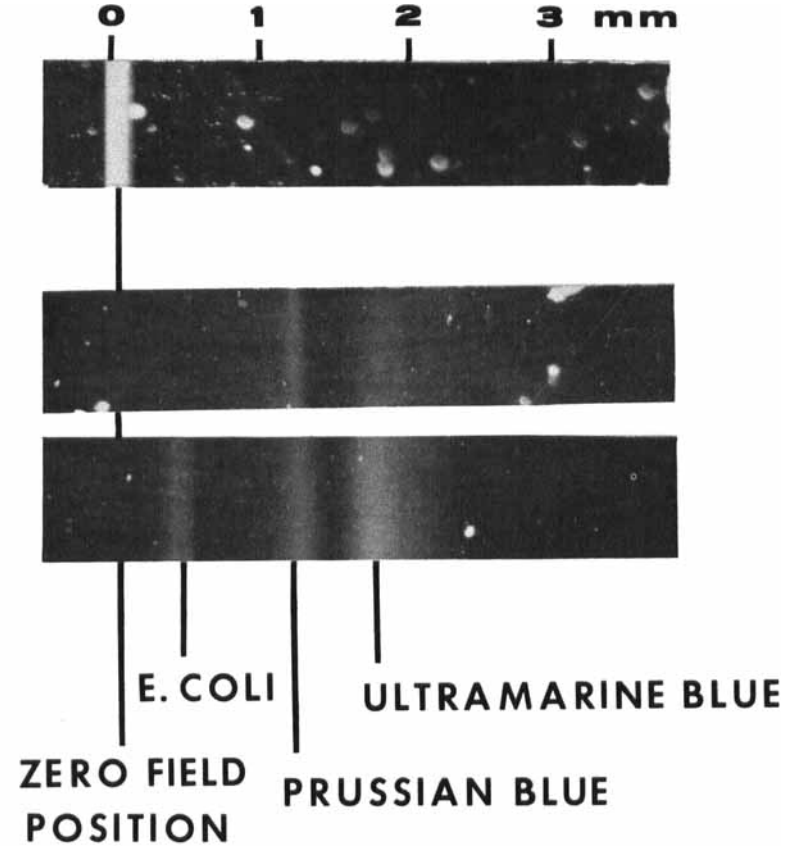

FIG. 3. Fractionation patterns: *E. coli* and mixed inorganics. Positive electrode at right. Medium: 0.003 *M* phosphate buffer, pH 6.1. Vertical transit path 11.4 cm, vertical transit velocity 1.6 cm/sec. Field gradient 78 volts/cm. Sample flow rate approx. 0.03 ml/min. Broad band for ultramarine blue is due to its chemical nonhomogeneity.

range from 1 μliter/min to about 0.2 ml/min. With usual curtain flow rates and a typical specific conductance of the medium of 260 μmhos, the field gradient may approach 70 volts/cm before special cooling provision is required.

Figure 3 shows some fractionation patterns as photographed at the lower end of an earlier, 2.5-cm-wide cell.

PERFORMANCE CONSIDERATIONS

The new performance capability stems in part from a remarkable combination of advantages found in a rapid, thin, narrow curtain. At velocities of the order of 1 cm/sec, manyfold higher than customary in two-dimensional methods, the curtain is strikingly stable against convective disturbance. The streamline pattern, seen in sample band behavior, is almost microscopically steady (within ±30 μ for a given sample run; ±50 μ long term). Relatively high settling rates of large or high-density particles are readily tolerated, since this rate may be small compared with curtain velocity. Electrical heating and temperature rise are kept low by the short residence time of any curtain element within the field. For a given voltage gradient, the required applied voltage for a narrow cell is low; and total dissipated wattage over the cell area is likewise low. There are important operating advantages also. The narrow cell allows us to introduce curtain electrolyte into the cell at a single inlet (and remove it from a single outlet if we wish), while maintaining a steady flow distribution across the curtain. The narrow cell is easy to build, and spacing between the plates is stable and easily reproduced following cell disassembly. The narrow cell may be conveniently scanned photoelectrically for recording the electrophoresis pattern.

Most important, the rapid curtain narrows the sample suspension (at the point of injection) to a very fine band even at moderately high sample flow rates. Provided broadening effects during the migration period are likewise small, the narrow sample band makes possible an extremely short response or analysis time. This stems from the fact that the time for completing an analysis is that required to separate the two components of least mobility difference. The smaller their bandwidth, the less the required time. Expressed differently, the achievement of a given resolution in any portion of the electrophoretic spectrum is equivalent to reducing to a certain minimum the ratio of bandwidth to band migration. This ratio

typically improves with time, and the required time is, again, less when the original bandwidth is less.

In the following we examine more closely the interplay of bandwidth determining factors, resolution, and analysis speed.

General Considerations

Assume we are viewing the band pattern across a horizontal line or slit at the lower end of the cell. Component bonds are visible, of certain width, at different displacement distances from an initial or zero position. It is convenient to define a *specific resolution* f_b, for any given band:

$$f_b = B/L_c$$

where B is bandwidth and L_c the lateral deflection.

Another convenient measure, which we may term *specific spectral resolution*, f_w, is given by

$$f_w = B/L_t$$

where L_t is the total spectrum width or range.

Any given component has been migrating laterally a time t, equal to the vertical transit time through the curtain. Lateral migration is proportional to t, and the attained bandwidth B equals the original bandwidth B_0 (at time of injection) plus broadening due to certain time-dependent effects. Particularly significant are *diffusion broadening*, B_d (for which in the following we take a root-mean-square value), and *velocity-profile broadening* B_{vp}. Expressing the relationships in simplified form, where k_1 to k_4 are proportionality constants:

$$L_c = k_1 t \tag{1}$$

$$B_0 = k_2 \tag{2}$$

$$B_d = k_3 t^{1/2} \tag{3}$$

$$B_{vp} = k_4 t^{*} \tag{4}$$

$$B = B_0 + B_d + B_{vp}$$

Each of the bandwidth terms is discussed in detail later.

* This assumes that the contribution to velocity-profile broadening by diffusion *in depth* is negligible. This assumption is valid even for relatively large values of initial bandwidth B_0 and relatively large diffusion constants. See the section below on velocity-profile broadening.

The specific resolution is given by

$$f_b = \frac{1}{k_1 t}\,(k_2 + k_3 t^{1/2} + k_4 t)$$

or

$$f_b = \frac{k_2}{k_1}\,t^{-1} + \frac{k_3}{k_1}\,t^{-1/2} + \frac{k_4}{k_1} \tag{5}$$

As t increases, specific resolution improves, diminishing in principle toward k_4/k_1 as a limit. Fortunately, as we shall see, k_4/k_1, the relative velocity-profile effect, will usually be quite small (with zero value as a special case). To optimize resolution, both the first and the second terms—relative original bandwidth and diffusion broadening—should likewise be made small, if possible as small as, or smaller than, k_4/k_1. It is found that the diffusion constants (proportional to k_3) for a wide gamut of particle size are small enough, that the second term in Eq. (5) can be made usefully small in a very short time t, usually of the order of a few seconds. This leaves only the first term, proportional to original bandwidth B_0, to be made small. This is made possible, as we mentioned, by the relatively high curtain velocity.

Migration Distance

Equation (1) may be written more explicitly as

$$L_c = (u_a + u_e)E(H/V_v) \tag{6}$$

where u_a is the electrophoretic mobility of a given band with respect to the bulk liquid, u_e is a lateral ("electroosmotic") mobility component of the liquid itself, and E is the electric field gradient. The factor H/V_v equals t, where H is the vertical height of the field acting on the particles and V_v is the vertical curtain velocity.

Since, according to Eq. (5), there is a time t beyond which specific resolution is not significantly improved (assuming finite k_4/k_1), it follows also that neither indefinite increase of cell height nor reduction of curtain speed will in general improve resolution *indefinitely*.

Since k_1 is proportional to E, we would expect from Eq. (5) an improved resolution with increase of E for a given t. However, as our later discussion shows, k_4/k_1, the relative velocity-profile broadening, also increases in proportion to E. Ultimate resolution is therefore not enhanced if velocity-profile broadening is finite.

Increased voltage will, however, reduce the time for attaining a given resolution.

The upper practical limit for E is set by thermal convection, which ultimately makes the bands too unstable either for observing band positions or collecting fractions. The upper limit for E is dependent, of course, on the conductivity of the curtain electrolyte, the transit time through the field, and certain features of the cell design. Without active cell cooling, a typical upper limit of field gradient in the present design has been 65 volts/cm, and typical corresponding upper values of deflection L_c have been about 10 to 15 mm.

Equation (6) states also that k_1 increases linearly with the particle mobility u_a. We can make no simple statement, however, on the effect of particle mobility on specific resolution, since u_a enters also into k_4. This relationship will be clarified later.

Sample Throughput and Bandwidth

The sample is usually injected into the curtain as a cylindrical jet. It is assumed as an approximation that it remains cylindrical as it descends with the curtain except for alteration of its form by broadening. The initial cross-sectional area (after the jet assumes the curtain velocity, within 1 mm or less of travel) is given by sample volume flow rate Q_s divided by curtain velocity V_{vc}. The original diameter or width of the band, B_0, is given by

$$B_0 = 2(Q_s/\pi V_{vc})^{1/2} \tag{7}$$

A compromise must therefore be made between minimum B_0, desirable for optimum resolution, and minimum desired sample throughput. Although V_{vc} can be increased for higher sample throughput, this is feasible only if the migration time t does not become too small.

At $V_{vc} = 1.0$ cm/sec, typical values in our work have ranged from $B_0 = 0.15$ mm at 0.01 ml/min sample flow, to $B_0 = 0.65$ mm at 0.2 ml/min sample flow.

As we shall show later, increase of sample flow rate also results generally in increased velocity-profile broadening, owing to increase in the fraction of film thickness occupied by the sample stream.

Diffusion Broadening

The root-mean-square lateral displacement of the particles caused by diffusion in time t is given by the Einstein relationship

$$\overline{\Delta X} = (2Dt)^{1/2}$$

where D is the diffusion constant. This constant is given by

$$D = RT/NF$$

where R is the gas constant, T is the absolute temperature, N is Avogadro's number, and F is a frictional constant. For particles large enough for Stokes' law to apply,

$$F = 3\pi\eta d_p$$

where η is the viscosity of the medium and d_p is the particle diameter. Broadening may accordingly be expressed as

$$\overline{\Delta X} = (2RTt/3\pi N\eta d_p)^{1/2} \tag{8}$$

TABLE 1

Diffusion Constants and Root-Mean-Square Displacements[a]

Particle	Diffusion constant, $D \times 10^7$ cm²/sec	$\Delta\bar{x}$, μ, at $t = 30$ sec
Sphere, 1 μ diam.	0.045[b]	5.1
Sphere, 0.1 μ diam.	0.45[b]	16
Nucleohistone (calf thymus), m.w. 2.3×10^6	0.93[c]	22
Globulin (human serum), m.w. 1.76×10^5	3.8[d]	48
Hemoglobin (human), m.w. 6.3×10^4	6.9[e]	65
Myoglobin, m.w. 1.7×10^4	11.3[f]	83
Glycine, m.w. 75	95[g]	240

[a] At 20°C.
[b] Calculated from Eq. (8).
[c] R. O. Carter, *J. Am. Chem. Soc.*, **63**, 1960 (1941).
[d] E. A. Kabat, *J. Exptl. Med.*, **69**, 103 (1939).
[e] O. Lamm and A. Polson, *Biochem. J.*, **30**, 528 (1936).
[f] A. Polson, *Kolloid-Z.*, **87**, 149 (1939).
[g] A. Polson, *Biochem. J.*, **31**, 1903 (1937).

Since our bands are broadened by diffusion both to the right and the left, a convenient approximate measure of the broadening is given by

$$B_d = 2\overline{\Delta X}$$

Table 1 shows the diffusion constants for particles ranging in size from a 1-μ-diameter sphere to a glycine molecule. Also shown are the root-mean-square displacements for a period of 30 seconds. Of interest is not only the very small displacement indicated for 1.0- or 0.1-μ particles, but the very slow increase of displacement with decreasing particle size. In principle, as in experimental fact, the variation of displacement with particle mass or molecular weight is of the order of the inverse fifth power. An important conclusion is that the advantages of the new technique should be applicable not only to microparticles, but to molecular species as well, of size at least as low-molecular-weight proteins.

Velocity-Profile Broadening

This important broadening effect appears not to have received critical attention. It stems from the fact that the sample material occupies a finite depth in the film. As such, it is subject to variations in vertical velocity, characteristic of the parabolic profile of laminar curtain flow. It is subject also to variations in a horizontal

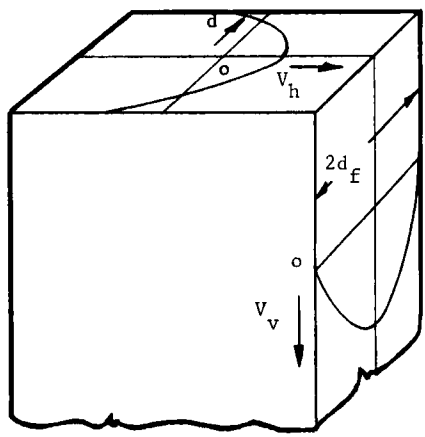

FIG. 4. Particle velocity profiles, horizontal and vertical, as function of depth (general case).

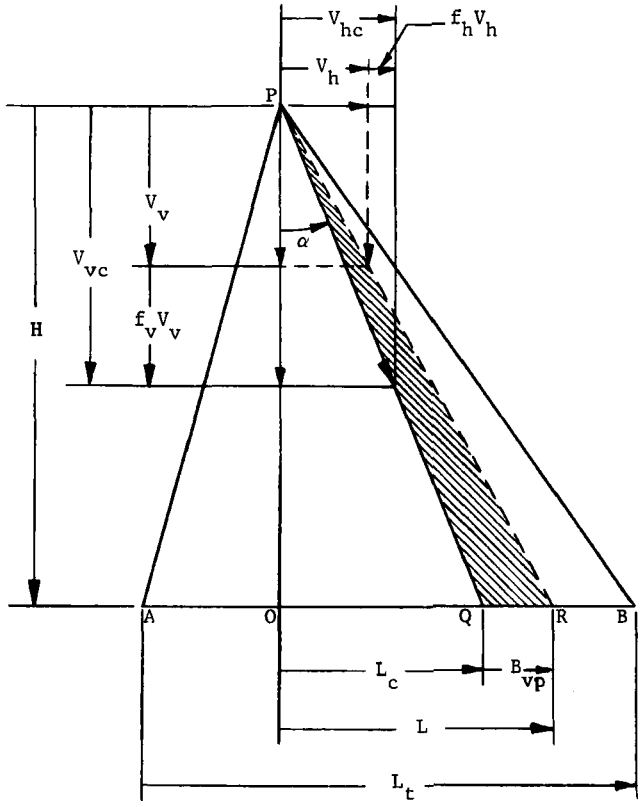

FIG. 5. Velocity and displacement relations in velocity-profile broadening.

component of curtain movement caused by electroosmotic streaming. The general appearance of these velocity profiles is shown in Fig. 4. This represents a small element of the flowing film, of half-thickness d_f, and shows the profiles in projection. (The vertical velocities as shown are much compressed, being in practice about a hundredfold larger than the horizontal.) The observed horizontal particle velocity V_h is the sum of the electroosmotic bulk flow velocity (of parabolic profile in the general case) and the electrophoretic particle velocity V_{ha} (constant at any depth for a given particle). The following examines the broadening B_{vp}, designated as *velocity-profile broadening*, caused by the composite effect of these vertical and horizontal velocity profiles.

It is assumed that vertical and horizontal velocity-profile effects

are independent, and act on the particles in simple superposition. As viewed in the figures, displacements to the right of the vertical axis (taken as the sample path at zero field gradient) are positive; those to the left negative. The positive direction for horizontal velocity and flow is to the right, and pressure increasing to the right is taken as a positive pressure gradient. It is assumed that settling of particles with respect to the fluid is negligible.

Figure 5 shows some relationships between particle velocity vectors and displacements as viewed from the front of the cell. Consider first a particle confined to the midplane of the curtain thickness and subject to a lateral electric field gradient. It has a vertical velocity vector V_{vc}, equal to the curtain midplane velocity, and a horizontal velocity vector V_{hc}, caused by electrophoretic and electroosmotic migration. Resultant particle motion is at an angle α from the vertical flow direction, given by

$$\tan \alpha = V_{hc}/V_{vc}$$

Continuous introduction at point P of a fine stream of particles of this same type produces a steady fine line along the direction PQ (assuming a uniform curtain velocity and field distribution). Viewing the electrophoretic "spectrum" along a horizontal line AB, at a distance H below P, a fine band is seen at Q, displaced a distance L_c from the axis PO. The displacement is given by

$$L_c = H(V_{hc}/V_{vc}) \tag{9}$$

Consider now a stream of the same particles no longer confined to the midplane, in consequence of finite thickness of the sample stream. Assume, for the marginal particles most displaced from the midplane, a fractional deviation $f_v V_{vc}$ in vertical velocity, and a deviation $f_v V_{hc}$ in horizontal velocity. This gives resultant velocities V_v and V_h, respectively, for such particles. The band at the viewing level is broadened to QR. This is the velocity-profile broadening B_{vp} defined earlier. Designating $(L_c + B_{vp})$ as L, the following relationships hold:

$$\frac{V_h}{V_v} = \frac{V_{hc}(1+f_h)}{V_{vc}(1+f_v)} = \frac{L}{H}$$

$$L = H\,\frac{V_{hc}(1+f_h)}{V_{vc}(1+f_v)} \tag{10}$$

It is useful to compare the broadening B_{vp} of a given particle band

with the full spectrum width L_t taken along AB. L_t corresponds to a total *range* V_{ht} in observed horizontal velocities for a given heterogeneous sample and is given by

$$L_t = H(V_{ht}/V_{vc}) \tag{11}$$

We now define a *fractional velocity-profile broadening* f_{bvp}:

$$f_{bvp} = B_{vp}/L_t = (L - L_c)/L_t \tag{12}$$

Substituting from Eqs. (9) to (11) in (12) and simplifying, we have

$$f_{bvp} = \frac{V_{hc}}{V_{ht}}\left(\frac{f_h - f_v}{1 + f_v}\right) \tag{13}$$

In the following we next define f_v and f_h as functions of the depth of particle extension into the film. The simplifying assumption is made that this extension is constant during particle transit through the curtain (i.e., that diffusion broadening in depth has negligible effect on velocity profile broadening, a generally valid supposition as indicated earlier). Extension to either side of the midplane will therefore generally be half the original bandwidth B_0.

The vertical velocity vector of the particle is that of the bulk liquid, a parabolic function of position in depth in the film (Fig. 4). From familiar fluid mechanical principles [see, for example, Bird et al. (*17*)], it may be shown that the velocity profile in our film, of thickness $2d_f$ which is small compared with the width W, is given by

$$V_v = (\Delta p_v/2\eta H)(d_f^2 - d^2) \tag{14}$$

where d is the distance from the midplane, Δp_v the dynamic vertical pressure differential over the interval H associated with vertical viscous flow, and η the viscosity.

From our definition of f_v we have

$$f_v = (V_v - V_{vc})/V_{vc} \tag{15}$$

Since V_{vc} is the value of V_v at $d = 0$,

$$V_{vc} = (\Delta p_v/2\eta H)d_f^2 \tag{16}$$

Substituting the values of V_v and V_{vc} from Eqs. (14) and (16) in (15), we obtain

$$f_v = -d^2/d_f^2 \tag{17}$$

To develop a corresponding function for f_h, we must examine the electroosmotic properties of a generalized cell of the present type. Figure 6 is a schematic horizontal section through the cell. The cell is assumed closed except for the membranes at the edges. The space outside each membrane may be considered a hydraulic "sink," such that addition of liquid to, or removal of liquid from, it by transfer through the cell does not alter the pressure in the sink. The thickness of the cell space, $2d_f$, is small compared with both W

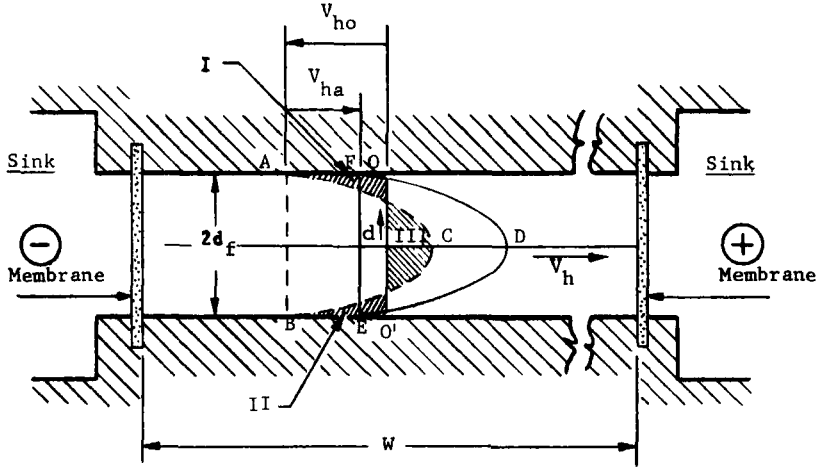

FIG. 6. Electroosmotic factors in horizontal velocity profiles.

and height H. It is assumed the walls have a certain potential ζ_w with respect to the bulk liquid. The latter therefore has a characteristic electroosmotic velocity V_{ho} at the wall given by the Helmholtz-Smoluchowski relationship:

$$V_{ho}/E = \zeta_w D_e/4\pi\eta$$

where D_e is the dielectric constant of the liquid and E the lateral electric field gradient.

In principle, the electroosmotic picture may vary between two extremes. This depends on the membrane properties, i.e., their impedance to mass flow and whether or not they act as electroosmotic "pumps" to influence transfer through the cell. At one extreme, assuming zero membrane impedance (i.e., zero pressure drop across the membranes), pressure at all points in a given horizontal plane in the cell is the same, and equal to pressure in the two sinks (assumed equal). Assuming the walls are negatively charged

and the positive electrode at the right, the cell liquid moves everywhere to the *left* in a form of plug flow (with zero viscous shear in the bulk liquid) at the velocity V_{ho}. This is represented by line AB in the figure, where OO' is the zero axis of lateral velocity. Particles with an electrophoretic velocity V_{ha} (with respect to the liquid) similarly have a straight velocity profile FE. The flow behavior is analogous to that of the classic capillary electroosmosis experiment, in the case where the ends of the capillary are "shorted" by an external loop permitting return flow. The nature of electroosmotic flow under these and other conditions was clarified by Smoluchowski (*18*).

At the other extreme, the membranes may be considered impermeable to mass flow, and net horizontal flow into or out of the cell is zero. This is analogous to the condition in microscope electrophoresis (*4*). The velocity contour for liquid flow is given by a parabolic curve ACB, satisfying the conditions that velocity at the walls is the characteristic electroosmotic velocity V_{ho}, and that the sum of shaded areas I + II (negative flow direction) equals area III (positive flow). The profile for particles of electrophoretic velocity V_{ha} is FDE, a parabola identical with ACB but displaced laterally by V_{ha}.

At intermediate conditions of membrane impedance, the liquid velocity profiles are a family of parabolas lying between AB and ACB. The velocity profiles for particles with electrophoretic velocity V_{ha} are parabolas between FE and FDE. The equations for these curves are derived on the same principles as for Hagen-Poiseuille flow through a narrow slit (*17*), except that boundary velocity at the wall is taken as V_{ho} instead of zero. The equations for these curves may be expressed in terms of a prevailing horizontal pressure differential Δp_h within the cell taken across the width W, or a prevailing horizontal rate of flow Q_h, into or out of the cell. The generalized equations for the observed particle velocity profiles are

$$V_h = (-\Delta p_h/2\eta W)(d_f^2 - d^2) + V_{ho} + V_{ha} \tag{18}$$

and

$$V_h = \left[\frac{3}{2d_f^2}\left(\frac{Q_h}{2d_f H} - V_{ho}\right)\right](d_f^2 - d^2) + V_{ho} + V_{ha} \tag{19}$$

wherein Δp_h and Q_h are related by

$$\Delta p_h = \frac{3\eta W}{d_f^2}\left(V_{ho} - \frac{Q_h}{2Hd_f}\right)$$

The particle velocity profile *FE* is that described by Eq. (18) at Δp_h equal to zero. The profile *FDE* is that described by Eq. (19) at Q_h equal to zero.

The fraction f_h by which horizontal velocity V_h deviates from midplane velocity V_{hc} is given by

$$f_h = (V_h - V_{hc})/V_{hc} \tag{20}$$

If the factor modifying $(d_f^2 - d^2)$ in either Eqs. (18) or (19) is designated as A, and for V_{hc} we take the value of V_h at $d = 0$, then we obtain from Eq. (18) or (19), plus (20),

$$f_h = -Ad^2/V_{hc} = -Ad^2/(Ad_f^2 + V_{ho} + V_{ha}) \tag{21}$$

We are now in a position to express f_{bvp}, Eq. (13), more explicitly. Substituting f_v and f_h from Eqs. (17) and (21) in (13) we obtain

$$f_{bvp} = \frac{d^2}{d_f^2 - d^2}\left(\frac{V_{ho} + V_{ha}}{V_{ht}}\right) \tag{22}$$

If we now express d as a fraction f_s of d_f, i.e., $d = f_s d_f$, we have

$$f_{bvp} = \frac{f_s^2}{1 - f_s^2}\left(\frac{V_{ho} + V_{ha}}{V_{ht}}\right) \tag{23}$$

Assuming that V_{ha} and V_{ho} are of positive and negative sign, respectively, when the wall and particle both have negative ζ potentials (ζ_w and ζ_a, respectively), Eq. (23) may also be expressed as

$$f_{bvp} = \frac{f_s^2}{1 - f_s^2}\left(\frac{\zeta_w - \zeta_a}{\zeta_t}\right) \tag{24}$$

where ζ_t is the total range of ζ potential in the electrophoretic spectrum, corresponding to the total particle velocity range V_{ht} or the spectrum width L_t.

For the absolute value of velocity-profile broadening, B_{vp}, we have from Eqs. (12) and (23),

$$B_{vp} = \frac{f_s^2}{1 - f_s^2}\left(\frac{V_{ho} + V_{ha}}{V_{ht}}\right) L_t \tag{25}$$

A useful alternative measure for velocity profile broadening is $f_{bvp'}$, the ratio of absolute broadening to *band displacement*. We may designate this as *specific fractional broadening* due to velocity

profile, given by

$$f_{bvp'} = \frac{f_s^2}{1 - f_s^2}\left(\frac{V_{ho} + V_{ha}}{V_{hc}}\right) \tag{26}$$

In this equation the expression in parentheses is simply the ratio of the velocity the particle would exhibit at the wall to that observed at the midplane.

In Eqs. (23) to (25) the terms in parentheses have a maximum possible value of unity if the ζ potential of the wall lies within the ζ potential range of the particles comprising the spectrum.

Conclusions to be drawn from Eqs. (23) to (26) are:

1. Velocity-profile broadening of bands in a spectrum will have varying values, but with a given cell and given operating conditions the broadening varies linearly with lateral displacement, i.e., with particle mobility or ζ potential.

2. Except when $\zeta_a \simeq \zeta_w$, a high premium in performance is gained by confining the sample to a moderate fraction f_s of the curtain thickness. (Unless f_s and velocity-profile broadening are small enough relative to original bandwidth B_0 and diffusion broadening B_d, resolution will be velocity-profile-limited. Specific resolution f_b will then be equal to about f_{bvp} at best. In usual practice, $f_s = \frac{1}{10}$ to $\frac{1}{3}$.)

3. Velocity-profile broadening is zero for particle bands such that $\zeta_a = \zeta_w$, independent of the value of f_s. In effect, horizontal and vertical profile effects are then mutually compensating. Both particle velocity profiles are parabolas with zero value at the wall, and at any depth d, horizontal and vertical velocities are in constant ratio, giving a unique resultant band direction (Fig. 5).

4. Fractional velocity-profile broadening is independent of the vertical curtain velocity.

5. Velocity-profile broadening relative to the spectral width is independent of net horizontal flow through the cell, or horizontal internal pressure differential across the cell.

ELECTROPHORETIC MOBILITY MEASUREMENT

In the following we consider briefly the question of making absolute electrophoretic mobility measurements by the continuous electrophoresis technique. By rearrangement of Eq. (6), we have for the particle mobility,

$$u_a = (L_c V_v / EH) - u_e$$

It is characteristic of the method that the primary measurement, the deflection L_c, can be made rapidly, conveniently, and precisely. Use of the equation implies that vertical flow and field gradient are uniform in the space traversed by the particles, and that the electroosmotic mobility component u_e is ascertainable.

The flow is in fact known to be quite uniform, from measurement of particle front velocities at different lateral positions in the field. The uniformity of the electric field has not been explored in detail; however, particle deflections are observed to vary linearly with the field gradient. The latter is measured by a pair of electrodes inserted at the edges of the curtain. Fringe effects do occur at the upper and lower ends of the field space. However, it is not inconvenient to measure a $\Delta L_c/\Delta H$ for purposes of the equation above, i.e., to measure a differential deflection within the uniform field space only.

The electroosmotic effect differs from that in microscope electrophoresis, in the sense that there is no plane (at a defined depth in the film) where electroosmotic flow is in principle zero. In the continuous technique this flow is dependent on the ζ potential of the cell wall, and may be influenced by electroosmotic effects in the membranes. Preliminary tests with substances of presumed zero mobility indicate a near-zero electroosmotic velocity at the cell midplane. In principle, effects at the cell wall and membrane may compensate each other to bring this about. The phenomenon requires further study, however. Meanwhile, reference substances may be used (5) to determine the zero of the mobility scale as well as to verify its slope.

The cell design has sought, in general, to improve factors such as resolution, speed, and throughput rather than to perfect the measurement of absolute mobility as such. Nevertheless it will be found very useful for many mobility studies, where its precision (±1 to 2%), long-term reproducibility (±2%), convenience, and speed will be valuable assets.

REFERENCES

1. N. G. Anderson, *J. Phys. Chem.*, **66**, 1984 (1962).
2. H. Mueller, in *Proteins, Amino Acids and Peptides* (E. J. Cohn and J. T. Edsall, eds.), Reinhold, New York, 1943, Chap. 25.
3. A. E. Alexander and P. Johnson, *Colloid Science*, Oxford, London, 1949.
4. C. C. Brinton, Jr., and M. A. Lauffer, in *Electrophoresis* (M. Bier, ed.), Academic Press, New York, 1959, Chap. 10.

5. H. A. Abramson, *Electrokinetic Phenomena and Their Application to Biology and Medicine,* Chemical Catalog Co., New York 1934; available as reprint from University Microfilms, Ann Arbor, Mich.
6. H. A. Abramson, L. S. Moyer, and M. H. Gorin, *Electrophoresis of Proteins,* Reinhold, New York, 1942; available as reprint from University Microfilms, Ann Arbor, Mich.
7. A. Kolin, *Proc. Natl. Acad. Sci. U.S.*, **46,** 509 (1960).
8. A. Kolin, *Proc. Natl. Acad. Sci. U.S.*, **41,** 101 (1955).
9. H. C. Mel, *J. Theoret. Biol.*, **6,** 159, 307 (1964).
10. A. Kolin, *J. Appl. Phys.*, **25,** 1442 (1954).
11. H. Hjerten, in *Protides of the Biological Bluids, Proc. 7th Colloq., Bruges,* Elsevier, Amsterdam, 1959, pp. 28–30.
12. V. J. Barrolier, E. Watzke, and H. Gibian, *Z. Naturforsch.*, **13b,** 754 (1958).
13. K. Hannig, *Z. Anal. Chem.*, **181,** 244 (1961).
14. K. Hannig, *Habilitationsschrift, Eine Neuentwicklung der trägerfrein Ablenkungselektrophorese und ihre Anwendung auf zytologische Probleme,* Max-Planck-Institut fur Eiweiss-und Lederforschung, Munich, 1964.
15. Reports of Beckman Instruments, Inc., to Space General Corp., El Monte, Calif., Contract DA-18-064-AMC-137A.
16. A. Strickler, A. Kaplan, and E. Vigh, *Microchem. J.*, **10,** 529 (1966).
17. R. B. Bird, W. E. Stewart, and E. W. Lightfoot, *Transport Phenomena,* Wiley, New York, 1960, Chap. 2.
18. N. V. Smoluchowski, *Bull. Intern. Acad. Polon. Sci. Classe Sci. Math. Nat.*, **1904,** 184.

Received by editor January 11, 1967
Submitted for publication January 25, 1967